Journal of Applied Spectroscopy, Vol. 91, No. 3, July, 2024 (Russian Original Vol. 91, No. 3, May–June, 2024)

MECHANISM OF PHOTODAMAGE OF MICROBIAL CELLS SENSITIZED BY INDOTRICARBOCYANINE DYE

A. A. Tabolich,[a] A. I. Tretyakova,[a] L. G. Plavskaya,[a] T. S. Ananich,[a] R. K. Nahorny,[a] V. Y. Plavskii,[a] L. S. Lyashenko,[b] E. S. Voropay,[b,*] and A. P. Lugovski[c]

UDC 535.37:(547.979.733+667.211.43)

The mechanism of photodamage of E. coli Gram-negative bacterial cells sensitized with indotricarbocyanine dye PK220 was studied upon exposure to radiation from an LED source with emission spectrum maximum wavelength λ_{max} = 745 nm corresponding to the long-wavelength absorption band of the dye. The intensity of the cells' own (not enhanced by activator additives) light-induced chemiluminescence was used to assess the magnitude of the photobiological effect. The main contribution to their photodestruction immediately after cessation of cell-suspension irradiation came from singlet oxygen and to a lesser extent from H_2O_2. Hydroxyl radicals did not play a significant role in the mechanism of sensitized photochemical processes.

Keywords: *indotricarbocyanine dye, photosensitizer, E. coli Gram-negative bacterial cells, antimicrobial photodynamic therapy, reactive oxygen species, chemiluminescence.*

Introduction. Photodynamic therapy (PDT) is currently considered a prospective and effective treatment for malignant tumors and an alternative and highly promising method for treating localized infections (antimicrobial PDT) [1–5]. These PDT methods involve preliminary parenteral administration of a dye sensitizer that accumulates primarily in tumors or stains the inflammation site by irrigation or applications followed by irradiation with a laser or LED source, the spectral composition of which corresponds to the sensitizer absorption spectrum. Indotricarbocyanine dyes are a promising class of sensitizers for use in medical PDT [1, 6]. Such compounds have high photodynamic activity and are characterized by strong absorption in the so-called transparency window of biological tissues (far red spectral region), providing deep penetration of the light into tissue. The delivery of high-intensity light deep into tissue is critical for the destruction of tumors and for the inactivation of pathogenic microorganisms because pathogens can reside in tissues to depths of 6 mm [7].

A synthetic scheme and laboratory setup for producing a new indotricarbocyanine photosensitizer (PS) have been elaborated and a protocol for a dosage form of the water-soluble PS PK220 has now been developed at A. N. Sevchenko Institute for Applied Physical Problems, Belarusian State University (Minsk, Belarus) [1]. Comprehensive studies of the PS photophysical and photochemical properties in solutions of various polarities and in healthy and neoplastic tissues of experimental animals have been performed [8–12]. The pharmacokinetic uptake and elimination of this dye from muscle and tumor tissue after intravenous administration were studied using spectral methods. The photodamage of grafted tumors in animals was characterized [13, 14]. The new PS was shown to exhibit high antitumor photodynamic activity, selective uptake, and low toxicity [15]. The indotricarbocyanine dye was demonstrated to sensitize the inactivation of microbial cells [16]. However, the mechanism of the photochemical processes initiating photodamage of biological structures after their sensitization by this compound are not clearly understood. It is known that indotricarbocyanine dyes can generate singlet oxygen [17–20], although the $^1O_2$ quantum yield is insignificant with φ_Δ = 0.03–0.10.

The aim of the present work was to study the photodestruction mechanism of microbial cells sensitized by the prototype dosage form of the water-soluble indotricarbocyanine dye PK220 with irradiation by an LED source, the spectral

*To whom correspondence should be addressed.

[a]B. I. Stepanov Institute of Physics, National Academy of Sciences of Belarus, Minsk, Belarus; email: v.plavskii@ifanbel.bas-net.by; [b]Belarusian State University, Minsk, Belarus; email: voropay@bsu.by; [c]A. N. Sevchenko Institute for Applied Physical Problems, Belarusian State University, Minsk, Belarus. Translated from Zhurnal Prikladnoi Spektroskopii, Vol. 91, No. 3, pp. 444–453, May–June, 2024. Original article submitted January 9, 2024.

range of which corresponded to the long-wavelength absorption band of the studied dye. The test for damage by the light was our own chemiluminescence (CL) method (not enhanced by activator additives). Addition before the studied biological media were irradiated of selective quenchers and scavengers of reactive oxygen species (ROS) showed that this method could identify the types of ROS involved in photochemical processes in cells [21–23].

Experimental. The water-soluble symmetric indotricarbocyanine dye PK220, which was developed at A. N. Sevchenko Institute for Applied Physical Problems, Belarusian State University, was studied. It is characterized by rather high water-solubility and biocompatibility because its structure includes hydrophilic substituents, e.g., two poly(ethylene glycol) moieties with molecular mass 300. The purity of the synthesized dye was monitored by the manufacturer using chromatography–mass-spectrometry and absorption, fluorescence, and fluorescence excitation spectra [13–15]. A concentrated dye stock solution, from which the corresponding additives to the cell suspension were prepared, was prepared in distilled water on the day of the experiment.

The damage by light was studied against *E. coli* M-17 Gram-negative bacterial cells (OAO Ferein, Belarus) with sensitization of them by PK220. Gram-negative bacteria were chosen as the subject of sensitized photodamage because their specific membrane structure presented a much greater problem for photoinactivation than that of Gram-positive bacteria [24, 25]. Triton-soy agar was used for cultivation of the microorganisms. The photodamaging action of the radiation was studied against cells grown for 24 h at 37^{o}C. The microorganism cultures were used in the exponential growth phase. The cells were rinsed with sterile normal saline (0.9% NaCl solution) after they were grown. Then, a cell suspension in normal saline was centrifuged for 10 min at 2150 g. The supernatant liquid was removed. The rinse procedure using normal saline to remove residual growth medium was repeated twice, removing the supernatant each time.

A bacterial suspension with a concentration of $1 \cdot 10^9$ cells/mL in sterile normal saline was prepared for irradiation of the cells. The cell concentration was estimated using an optical turbidity standard.

The damaging action of the light was studied by placing cell suspension (220 μL) into flat-bottomed cylindrical glass tubes of inner diameter ~14 mm. The suspension was treated 3 min before irradiation with concentrated PK220 solution (20 μL). This time was strictly observed in all tests because subsequent experiments showed that the cell incubation time with the dye had a significant influence on the magnitude of the photobiological effect. For this reason, the photodamaging effect was studied in separate specially arranged experiments as a function of dye incubation time with the cells.

The tube contents with added dye were thoroughly mixed and irradiated by a red LED through the cuvette bottom. The final dye concentration in the suspension was 1.5 μM. The optical density in a 1-cm cuvette at the absorption band maximum of λ_{max} = 706 nm was A = 0.72. The optical density of the dye at its absorption band maximum was $A \le 0.15$ because the thickness of the cell suspension was ≤2 mm. The value near the emission maximum of the LED spectrum was $A \le 0.05$.

Absorption spectra during preparation of dye solutions and the cell suspension were measured on a Cary-500 Scan UV-Vis-NIR spectrophotometer (Varian, USA–Australia) using standard quartz cuvettes (10 × 10 × 40 mm).

The cell suspension was irradiated by an LED operating in continuous mode with an emission spectrum maximum at λ_{max} = 745 nm. The LED emission power was varied by changing the current.

Figure 1 shows normalized spectra of the aqueous dye solution absorption and the LED emission. The LED emission was observed to lie on the long-wavelength edge of the PK220 absorption band. As shown before [1, 13, 14], the use of long-wavelength radiation increases the depth of pathological site photodestruction upon treating biological tissue with light. The irradiation time of the cell suspension was t = 1–10 min. The power density of the active radiation was I = 3–150 mW/cm^2. The power density of the radiation at the upper surface of the liquid column was monitored using a PM100D meter with an S121C photodiode sensor (Thorlabs GmbH, Germany).

The magnitude of the photobiological effect was characterized by monitoring the CL of the cell suspension itself (not enhanced) after preliminary irradiation. The CL method is known to be rather sensitive because it can simultaneously (summed) record various ROS (including superoxide anion radical .., H_2O_2, and hydroxyl radical $OH^{\bullet}$) located both within and outside cells. The cell emission parameters were measured on a Lum 5773 chemiluminometer (DISoft, Russia) operating in photon counting mode with spectral sensitivity 300–650 nm. CL signals were recorded and processed using specialized software.

After the irradiation was stopped, the suspension was immediately transferred to a chemiluminometer cuvette. The time from the cessation of irradiation of the suspension to the start of recording the CL signal was strictly controlled at 24 s. Analogous manipulations (except for the irradiation) were performed with control suspension samples. The CL measurements of control (unirradiated) and test samples of cell suspensions were alternated in an arbitrary order. CL (in

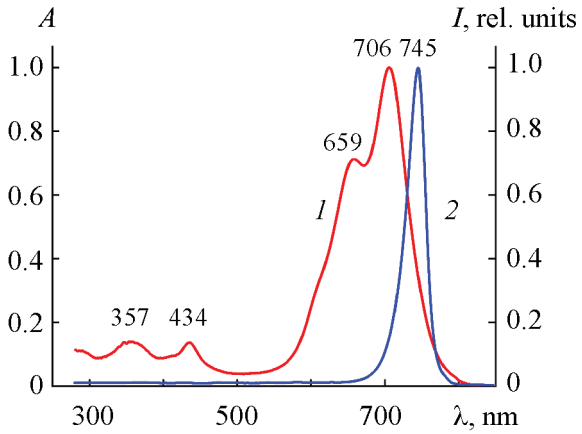

Fig. 1. Normalized absorption spectrum of indotricarbocyanine dye PK220 dosage form in deionized water (1) and emission spectrum of LED matrix (2).

relative units) was measured using a luminometer at 22°C. The CL signal was characterized using the light sum (S_{CL}), i.e., the area under the emission intensity curve for 5 min after the start of recording.

One of the specific quenchers (scavengers) of ROS (sodium azide, a singlet oxygen quencher; sodium pyruvate, an H_2O_2 scavenger; mannitol or DMSO, hydroxyl radical scavengers; and the universal antioxidant quercetin, a superoxide radical, hydroxyl radical, H_2O_2, and singlet oxygen scavenger [27, 28]) (10 μL) was added to the cell suspension 10 min before the irradiation to clarify the type of ROS involved in the photochemical processes in cells sensitized by PK220 upon irradiation by red light. The concentrations of the stock solutions (concentrated) of these quenchers (scavengers) were adjusted so that the final concentration after adding 10 μL of one of them to cell suspension with dye (220 μL) would be 10 mM for sodium azide and sodium pyruvate, 50 μM for quercetin, 40 mM for mannitol, and 1 M for DMSO. Samples of cell suspension without the ROS quenchers were diluted with normal saline (10 μL). Cell suspensions with and without ROS quenchers were treated 3 min before irradiation with a concentrated solution of PK220 (20 μL) so that its final concentration was 1.5 μM. Cell suspensions with and without ROS quenchers and scavengers were irradiated for t = 3 min by red light with I = 100 mW/cm^2 (energy dose D = 18 J/cm^2). Their effects on S_{CL} were evaluated.

Results and Discussion. The CL intensity of unirradiated PK220 dye solutions, an intact suspension of microbial cells, and cell suspension with dye was characteristically low and practically did not change during recording for 5 min. Figure 2a shows the kinetic curve reflecting the change with time of the CL signal of a suspension of unirradiated *E. coli* cells (concentration $1 \cdot 10^9$ mL^{-1}) with PK220 dye (1.5 μM). The CL signal also practically did not change after irradiation by light with λ_{max} = 745 nm of the cell suspension without dye or dye solution without cells.

Figure 2b shows the change with time of the CL signal of a suspension of *E. coli* cells (concentration $1 \cdot 10^9$ mL^{-1}) without dye after irradiation by light with λ_{max} = 745 nm and power density I = 50 mW/cm^2 for t = 3 min (D = 9 J/cm^2). The data show that the ROS concentration was not sufficient to increase the CL signal upon recording the CL for 24 s after irradiation of the cell suspension or dye in normal saline. The situation was different after irradiation with the above parameters of a suspension of *E. coli* cells sensitized by PK220 dye (Fig. 2c). The kinetics of the change of CL intensity was a descending curve after incubation of the dye with cells for 3 min followed by irradiation of them. The CL intensity 5 min after the start of recording was significantly greater than the level of the unirradiated control of this suspension, confirming the presence of dark chemical processes initiated in the studied system by irradiation.

As noted, the intensity of light-induced CL of sensitized cells depended on their incubation time with PK220 dye with constant parameters of the active radiation. Figure 3 shows the dependence of light sum S_{CL} induced by light with λ_{max} = 745 nm of power density I = 50 mW/cm^2 for t = 3 min (D = 9 J/cm^2) on the duration of preliminary incubation of the dye with the cell suspension. The maximum intensity of light-induced CL was observed after 3 min of incubation of the dye with the cells before the start of irradiation. The CL signal decreased smoothly as the incubation time increased and reached a constant level that was 1.8 times less than the maximum. The observed dependence of light-induced CL intensity on incubation time of the dye with the cell suspension could be explained by a change in the location of the dye in the cell structure, primarily in their membrane, because incubation of the dye with the cells for 120 min did not noticeably change

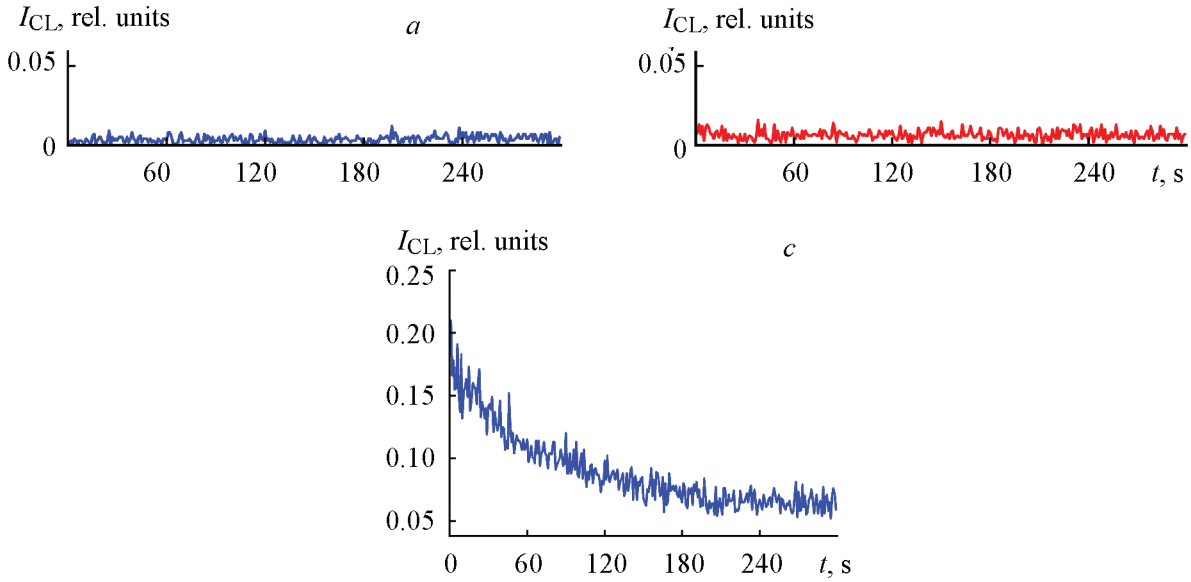

Fig. 2. Kinetic curves of CL intensity of suspension of *E. coli* cells in normal saline: with PK220 without irradiation (a), after irradiation without PK220 (b), after irradiation of cell suspension with PK220 (c); cell concentration $1 \cdot 10^9$ mL^{-1}, PK220 concentration 1.5 μM, λ_{max} = 745 nm, I = 50 mW/cm^2, t = 3 min, D = 9 J/cm^2.

Fig. 3. Dependence of light sum of CL induced by light with λ_{max} = 745 nm, power density I = 50 mW/cm^2 for t = 3 min (D = 9 J/cm^2) on time of preliminary incubation of PK220 dye with cell suspension.

the absorption spectrum of PK220. The cell wall structure of Gram-negative bacterium *E. coli* is known to be 14–18 nm thick [29]. It is divided into an external (outer) membrane and a thin peptidoglycan layer (murein sacculus). The external membrane of *E. coli* is a phospholipid bilayer containing proteins and lipopolysaccharides. The external membrane is connected to the underlying peptidoglycan layer through a membrane lipoprotein. The peptidoglycan of Gram-negative bacteria is a monolayer (2–3 nm thick), under which the cytoplasmic membrane is located. A void (periplasmic space or periplasm) ≤10 nm thick exists between the external membrane, peptidoglycan layer, and cytoplasmic membrane. This space is filled with a gel containing transporter proteins and enzymes. This complicated cell-membrane structure in Gram-negative bacteria is thought to be the reason for their higher resistance than Gram-positive microorganisms to sensitized photodamage involving exogenous compounds. Therefore, it could be expected that the increase in the intensity of light-induced CL of the cell suspension in the first 3 min of incubation with PK220 was due to an increase in the number of dye molecules incorporated into the outer membrane and with a high probability of inducing in it photochemical reactions during irradiation. However, some of the dye molecules redistributed into other sections of the cell wall as the incubation time increased. This was probably associated with the reduction in the efficiency of the photochemical reactions and a corresponding reduction in the level of formed ROS and CL intensity. In turn, the reason for the reduced probability of photodamage of internal structures of the cell membrane may be both localization of the dye in a region of molecular structures less sensitive to photodamage and natural antioxidants (glutathione, riboflavin, flavonoids, amino acids, antioxidant enzymes, etc.) situated next to the PS.

It seemed interesting to determine the optimum PK220 concentration for inducing the maximum CL signal. Figure 4 shows the dependence of S_{CL} of light-induced CL on the dye concentration for a constant concentration of sensitized microbial cells after irradiation for t = 3 min of their suspension by light with λ_{max} = 745 nm and power density I = 150 mW/cm^2 (D = 27 J/cm^2). The light sum of CL under our experimental conditions was observed to increase rapidly with increasing dye concentration in the range 0.2–1.0 μM, reaching a maximum for C = 1–2 μM. Apparently, the increase in the signal strength in the initial stage of the function $S_{CL} = f(C)$ was due to an increase in the number of dye molecules interacting with the microbial cells and a corresponding increase in the amount of photodamage of the cell structures during irradiation. Increasing the dye concentration further after reaching the maximum light sum led to a slow decrease in the CL

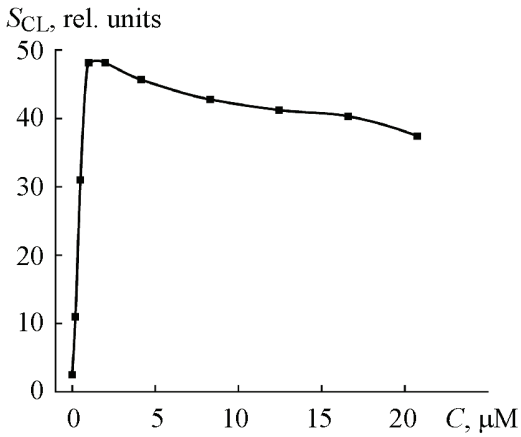

Fig. 4. Dependence of light sum of CL induced by light with λ_{max} = 745 nm, power density I = 150 mW/cm^2 for t = 3 min (D = 27 J/cm^2) on PK220 concentration in cell suspension.

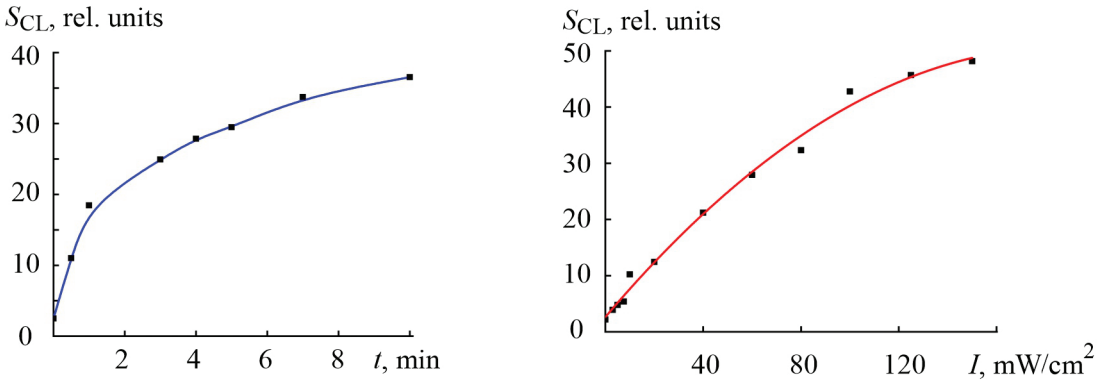

Fig. 5. Dependence of light sum of CL on irradiation time of *E. coli* cell suspension sensitized by PK220 dye by radiation with λ_{max} = 745 nm with constant power density I = 50 mW/cm^2.

Fig. 6. Dependence of light sum of CL on power density of radiation with λ_{max}= 745 nm irradiating for t = 3 min on *E. coli* cell suspension sensitized by PK220.

signal. Several reasons could be responsible for this decrease in the CL light sum with increasing dye concentration. First, shielding by the dye of the CL signal, the emission spectrum of which occurred in the visible region and depended strongly on the type of emitter involved in the emission [26, 30]. Second, quenching by the dye of ROS generated during PK220 photoexcitation. Third, the reduction in the CL light sum with increasing dye concentration could be related to a deficiency of molecular oxygen used for photodestruction of the microbial cells because it was burned up in the reaction with the PS.

It was important to demonstrate a relationship between the CL intensity and the parameters of the active radiation (its power density and exposure) to reveal the mechanism of the photochemical reactions sensitized by PK220 dye on the microbial cells. Figure 5 shows the dependence of S_{CL} on the irradiation time of the *E. coli* cell suspension sensitized by the dye with constant radiation intensity I = 50 mW/cm^2. Figure 6 shows the dependence of S_{CL} on power density of the active radiation for t = 3 min. The functions $S_{CL} = f(t)$ and $S_{CL} = f(I)$ differed. The former was characterized by a rapid increase in the CL signal for irradiation time t = 1–1.5 min after which the rate of increase of the CL light sum dropped noticeably with increasing irradiation time up to t = 10 min. A possible reason for the slowing of the increase in the CL signal was the competition of two processes, i.e., light-induced formation of primary and secondary ROS during dye photoexcitation

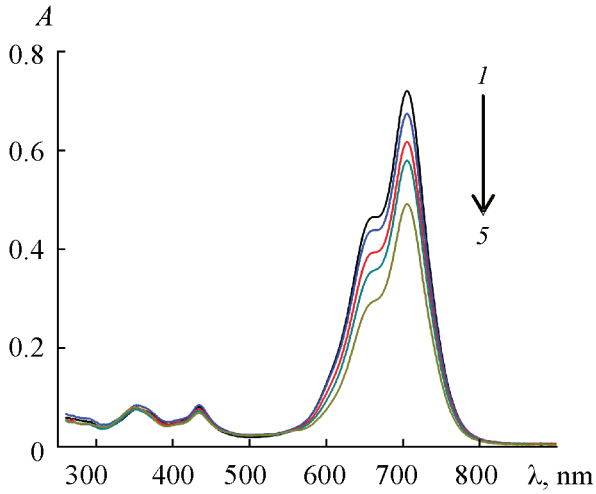

Fig. 7. PK220 dye absorption spectrum in normal saline irradiated by LED radiation with λ_{max} = 745 nm and power density I = 50 mW/cm^2 for t = 0 (1), 1 (2), 2 (3), 3 (4), and 6 min (5).

and ROS quenching upon their reaction with the cells and water during irradiation of the cell suspension. These reactions reached a steady state over time, which should have led to independence of the CL light sum on the irradiation time.

The function $S_{CL} = f(I)$ in the initial stage of light intensity growth was close to linear (Fig. 6). Then, the growth of the CL light sum slowed as the power density of the active radiation increased. One reason for the observed behavior was photodestruction of dye during its irradiation in the solution. Figure 7 shows absorption spectra of PK220 in normal saline upon irradiation by an LED source with λ_{max} = 745 nm and power density I = 50 mW/cm^2 for t = 1, 2, 3, and 6 min. The optical density at the PK220 absorption spectrum maximum for irradiation time t = 3 min (D = 9 J/cm^2) (curve 4) was observed to decrease by ~20%, which would naturally be reflected in the paths of the curves $S_{CL} = f(t)$ and $S_{CL} = f(I)$ (Figs. 5 and 6). Nevertheless, the presence of a pronounced dependence of the CL light sum on the energy dose of active radiation indicated that the CL light sum characterized the damaging action of the light on the microbial cells sensitized by PK220 dye.

The effect on the CL light sum of specific ROS quenchers (scavengers) (sodium azide, a singlet oxygen quencher; sodium pyruvate, an H_2O_2 scavenger; *D*-mannitol, a hydroxyl radical scavenger; and quercetin, a universal antioxidant capable of acting as a quencher of superoxide anion radical, hydroxyl radical, H_2O_2, and singlet oxygen) was studied to reveal the mechanism of photochemical reactions determining the photodamage of *E. coli* microbial cells sensitized by PK220 dye [27, 28]. Addition of these ROS quenchers (scavengers) to suspensions of microbial cells sensitized by PK220 dye without irradiation was shown to have practically no effect on the CL intensity, i.e., the change of CL intensity during signal recording for t = 5 min corresponded to that in Fig. 2a.

The presence of several of these ROS quenchers (scavengers) in a suspension of cells sensitized by PK220 was reflected in the intensity of light-induced CL as compared to the results for the same suspensions without the quenchers. Figure 8 compares the effects of ROS quenchers on the CL light sum of a suspension of *E. coli* cells sensitized to PK220 dye after irradiation by light with λ_{max} = 745 nm and power density I = 100 mW/cm^2 for t = 3 min. Addition to the cell suspension before its irradiation with PK220 of the hydroxyl radical scavenger *D*-mannitol or DMSO had practically no effect on the CL light sum. Therefore, hydroxy radicals did not contribute appreciably to the photodamage of *E. coli* microbial cells. However, addition of the universal antioxidant quercetin, a scavenger of superoxide anion radical, hydroxyl radical, H_2O_2, and singlet oxygen, before irradiation of the cells reduced the light sum of light-induced CL recorded without the quenchers by >3.5 times. Thus, singlet oxygen contributed significantly to damage sensitized by the dye of the microbial cells. For example, addition of sodium azide, a $^1O_2$ quencher, before irradiation of the cells reduced the light sum of light-induced CL by >1.8 times as compared to the CL light sum of irradiated samples without the quenchers. H_2O_2 contributed slightly to the photochemical reactions recorded in microbial cells sensitized by PK220 dye because addition before irradiation of the cells of an H_2O_2 scavenger (sodium pyruvate) reduced the intensity of light-induced CL by 1.4 times as compared to samples without the quencher.

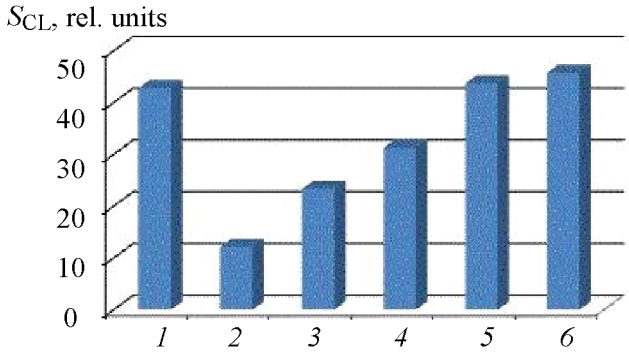

Fig. 8. Effect of ROS quenchers on CL light sum of *E. coli* cell suspension sensitized by PK220 dye after irradiation by radiation with λ_{max} = 745 nm and power density I = 100 mW/cm^2 for t = 3 min: without quenchers (1), with quercetin (50 μM) (2), with sodium azide (10 mM) (3), with sodium pyruvate (10 mM) (4), with *D*-mannitol (40 mM) (5), with DMSO (1 M) (6).

Thus, singlet oxygen acted as the main intermediate determining the photodamage of *E. coli* microbial cells in the presence of PK220 dye during irradiation by an LED source with λ_{max} = 745 nm, despite the relatively low quantum yield of its formation sensitized by the indotricarbocyanine dye (φ_Δ = 0.03–0.10) [17–20]. H_2O_2 also contributed somewhat to the photochemical damage of the microorganisms.

These trends in the photochemical reactions occurring in *E. coli* cells were studied immediately after stopping the irradiation. Literature data [21, 31] indicate that the mechanism of the light-induced reaction in the cells changed over time after the irradiation stopped because of secondary production of ROS, primarily H_2O_2. Figure 2a shows that the chemical reactions in the cells that were induced by light occurred for a rather long time. The intensity of light-induced CL of the cells 5 min after the irradiation stopped was significantly greater than the level of spontaneous CL. According to the literature [32], increased levels of H_2O_2 could be recorded in cells after their sensitized damage for ~80 min after irradiation. This time depended strongly on the type and location of the PS in the cells.

Conclusions. The CL method could quickly produce information about the photodamage mechanism of *E. coli* microbial cells sensitized by the indotricarbocyanine dye PK220. Studies could be performed with dyes or drugs with sensitizing properties and dark cytotoxicity, which is usually very complicated when studying the effects of sensitized damage of microorganisms by methods based on evaluating their ability to form colonies (colony-forming units). It was concluded based on a comparison of light sums of light-induced CL of suspensions of cells sensitized by PK220 dye with and without specific ROS quenchers (scavengers) that singlet oxygen was the main intermediate determining the damage to microbial cells during irradiation by an LED source with λ_{max} = 745 nm. H_2O_2 also contributed significantly to the studied photochemical reactions. Hydroxyl radical did not play a substantial role in photodamage of *E. coli* microbial cells, in contrast to these ROS. Quercetin, a universal antioxidant quenching ROS such as superoxide anion radical, hydroxyl radical, H_2O_2, and singlet oxygen, had the most pronounced protective effect on photodamage of the microorganisms among the examined ROS quenchers (scavengers) (sodium azide, sodium pyruvate, *D*-mannitol, DMSO, quercetin).

REFERENCES

1. A. A. Lugovski, M. P. Samtsov, K. N. Kaplevsky, D. Tarasau, E. S. Voropay, P. T. Petrov, and Y. P. Istomin, *J. Photochem. Photobiol., A*, **316**, 31–36 (2016).
2. G. Gunaydin, M. E. Gedik, and S. Ayan, *Front. Chem.*, **9**, Article ID 686303 (2021).
3. X. Hu, H. Zhang, Y. Wang, B. C. Shiu, J. H. Lin, S. Zhang, C. W. Lou, and T. T. Li, *Chem. Eng. J.*, **450**, Article ID 138129 (2022).
4. L. G. Astaf'eva, G. A. Zalesskaya, and V. Yu. Plavskii, *Opt. Spektrosk.*, **112**, No. 4, 697–702 (2012).
5. G. A. Zalesskaya, L. G. Astaf'eva, and V. Y. Plavskii, *J. Appl. Spectrosc.*, **79**, 288–295 (2012).
6. A. A. Ishchenko and A. T. Syniugina, *Theor. Exp. Chem.*, **58**, No. 6, 373–401 (2023).

7. M. Sanz, L. Lau, D. Herrerra, J. M. Morillo, and A. Silva, *J. Clin. Periodontol.*, **31**, No. 12, 1034–1047 (2004).
8. M. P. Samtsov, S. A. Tikhomirov, L. S. Lyashenka, D. S. Tarasau, O. V. Buganov, V. A. Galievsky, A. S. Stasheuski, and E. S. Voropay, *J. Appl. Spectrosc.*, **80**, 170–175 (2013).
9. N. V. Belko, G. A. Gusakov, S. K. Poznyak, S. A. Tikhomirov, A. P. Lugovski, and M. P. Samtsov, *J. Phys. Chem. C*, **126**, No. 18, 7922–7932 (2022).
10. N. V. Belko, M. P. Samtsov, G. A. Gusakov, D. S. Tarasau, A. A. Lugovski, and E. S. Voropay, *J. Appl. Spectrosc.*, **85**, 997–1005 (2019).
11. N. V. Belko, M. P. Samtsov, G. A. Gusakov, I. I. Khludeev, A. P. Lugovski, and A. A. Lugovski, *J. Appl. Spectrosc.*, **87**, 412–420 (2020).
12. N. V. Belko, M. P. Samtsov, S. A. Tikhomirov, and O. V. Buganov, *J. Appl. Spectrosc.*, **87**, 830–839 (2020).
13. M. P. Samtsov, D. S. Tarasov, A. P. Lugovskii, P. T. Petrov, A. O. Savin, R. D. Zil′berman, and E. S. Voropai, *Dokl. BGUIR*, **18**, No. 8, 5–13 (2020).
14. M. P. Samtsov, D. S. Tarasov, E. S. Voropai, L. S. Lyashenko, P. T. Petrov, V. M. Nasek, A. O. Savin, and R. D. Zil′berman, *Zh. Bel. Gos. Univ. Fiz.*, No. 1, 19–26 (2019).
15. M. P. Samtsov, D. S. Tarasov, A. P. Lugovskii, E. S. Voropai, R. D. Zil′berman, and A. O. Savin, *Medelectronics–2022. Medical Electronic Equipment and New Medical Technologies: Collection of Scientific Articles from the XIII Int. Scientific-Technical Conf.* [in Russian], December 8–9, 2022, Minsk, Belarusian State University of Informatics and Radioelectronics, BSUIR, Minsk (2022), pp. 149–153.
16. M. P. Samtsov, A. P. Lugovskii, A. A. Lugovskii, L. S. Lyashenko, E. S. Voropai, T. S. Ermakova, and L. P. Titov, *Water-Soluble Indotricarbocyanine Dye*, Pat. No. 18027, Feb. 28, 2014, *Afitsyiny Byull.*, No. 1, 96 (2014).
17. M. P. Samtsov, E. S. Voropai, K. N. Kaplevskii, and D. G. Mel′nikov, *J. Appl. Spectrosc.*, **75**, 692–699 (2008).
18. M. P. Samtsov, D. S. Tarasau, A. S. Stasheuski, K. N. Kaplevsky, and E. S. Voropay, *J. Appl. Spectrosc.*, **81**, 214–221 (2014).
19. K. N. Kaplevskii, M. P. Samtsov, A. S. Stashevskii, V. A. Galievskii, D. S. Tarasov, and E. S. Voropai, *Vestn. BGU, Ser. 1: Fiz. Mat. Inf.*, No. 2, 7–11 (2012),
20. M. P. Samtsov, D. S. Tarasov, and E. S. Voropay, *J. Appl. Spectrosc.*, **90**, 1029–1036 (2023).
21. V. Y. Plavskii, L. G. Plavskaya, O. N. Dudinova, A. I. Tretyakova, A. V. Mikulich, A. N. Sobchuk, R. K. Nahorny, T. S. Ananich, A. D. Svechko, S. V. Yakimchuk, and I. A. Leusenko, *J. Appl. Spectrosc.*, **90**, 334–345 (2023).
22. V. Y. Plavskii, N. V. Barulin, A. V. Mikulich, A. I. Tretyakova, T. S. Ananich, L. G. Plavskaya, I. A. Leusenka, A.N. Sobchuk, V. A. Sysov, O. N. Dudinova, A. I. Vodchits, I. A. Khodasevich, and V. A. Orlovich, *J. Photochem. Photobiol. B*, **216**, 112112 (2021).
23. V. Plavskii, A. Mikulich, N. Barulin, T. Ananich, L. Plavskaya, A. Tretyakova, and I. Leusenka, *Photochem. Photobiol.*, **96**, No. 6, 1294–1313 (2020).
24. E. S. Voropai, M. P. Samtsov, A. P. Lugovskii, A. A. Lugovskii, T. S. Ermakova, L. P. Titov, and T. N. Bakaev, *Zdravookhranenie*, No. 11, 45–47 (2006).
25. V. Yu. Plavskii, A. V. Mikulich, A. I. Tretyakova, I. A. Leusenka, L. G. Plavskaya, O. A. Kazyuchits, I. I. Dobysh, and T. P. Krasnenkova, *J. Photochem. Photobiol. B*, **183**, 172–183 (2018).
26. Yu. A. Vladimirov and E. V. Proskurina, *Usp. Biol. Khim.*, **49**, No. 7, 341–388 (2009).
27. K. Hirota, H. Tanaka, T. Maeda, K. Tsukagoshi, H. Kawakami, T. Ozawa, and M. Wada, *Mater. Sci. Appl.*, **14**, No. 10, 482–499 (2023),
28. Y. Hanasaki, S. Ogawa, and S. Fukui, *Free Radical Biol. Med.*, **16**, No. 6, 845–850 (1994).
29. T. Wu, A. C. McCandlish, L. S. Gronenberg, S. S. Chng, T. J. Silhavy, and D. Kahne, *Proc. Natl. Acad. Sci. USA*, **103**, No. 31, 11754–11759 (2006).
30. R. F. Vasil′ev, Yu. B. Tsaplev, and A. V. Trofimov, *Usp. Khim.*, **79**, No. 2, 91–103 (2010).
31. J. V. Kruchenok, O. N. Dudinova, and V. Y. Plavskii, *J. Biomed. Photonics Eng.*, **9**, No. 2, Article ID 020303 (2023).
32. N. Peskova, A. Brilkina, A. Gorokhova, N. Shilyagina, O. Kutova, A. Nerush, A. Orlova, L. Klapshina, V. Vodeneev, and I. Balalaeva, *J. Photochem. Photobiol. B*, **219**, Article ID 112208 (2021).